PHYSICAL REVIEW A **93**, 011802(R) (2016)

Slow-light-induced Doppler shift in photonic-crystal waveguides

K. Kondo and T. Baba
Department of Electrical and Computer Engineering, Yokohama National University, 79-5 Tokiwadai, Hodogayaku, Yokohama 240-8501, Japan
(Received 6 October 2015; published 25 January 2016)

In this Rapid Communication, we theoretically discuss a large Doppler shift in a signal slow-light pulse in a photonic-crystal waveguide by considering its reflection at a quasilight speed mirror. The mirror is formed by the photonic band-gap shift induced by the high nonlinearity of a control slow-light pulse, which could be possible in a realistic device. In the simulation, the Doppler shift appears at multiple frequencies due to the Bloch nature of the photonic lattice. Larger but inefficient Doppler shifts occur through nonadiabatic processes, whereas the smallest but more efficient shift (i.e., the intraband Doppler shift) occurs through an adiabatic process. The occurrence of the intraband shift depends on whether the adiabatic process produces a complete reflection of the incident pulse, despite the fact that the pulse penetrates the mirror. A large band-gap shift and a moderately slow mirror satisfy this condition; otherwise, the shift ends at the halfway point.

DOI: 10.1103/PhysRevA.93.011802

I. INTRODUCTION

Optical interactions, such as cross-phase modulation and parametric frequency conversion, occur when two light waves with different wavelengths propagate together. However, the collision of two light waves and the resulting reflection have yet to be fully discussed. It is of great interest to consider how such a situation can be produced and what phenomena result. In a related theoretical study, the Doppler shift in a terahertz wave, which is reflected by a moving mirror formed by light absorption, is demonstrated [1]. The acousto-optic modulation is known to be an application of the Doppler shift of light induced by the reflection at moving acoustic waves. This phenomenon is also theoretically discussed with a photonic-crystal device [2,3]. However, the Doppler shift is small because the velocities of acoustic waves are on the order of $10^{-5}\,c$, much slower than the velocity of light c. Recently, Ulchenko *et al.* published a theoretical discussion on pulse compression through a Doppler shift, supposing a moving mirror with a conceptual index change [4]. In this study, we considered the possibility of a large Doppler shift using a slow-light-induced mirror formed in a realistic manner.

To date, we have demonstrated fast delay tuning, adiabatic wavelength conversion, and temporal pulse compression using signal and control slow-light pulses propagated together in a lattice-shifted photonic-crystal waveguide (LSPCW), which we referred to as a copropagating slow-light system [5–7]. In these studies, a Si LSPCW and pulses at telecom wavelengths were used so that the control pulse generates carrier plasma dispersion induced by two-photon absorption (TPA) [8], which is enhanced by low-dispersion slow light. In this study, we considered another situation wherein two pulses propagate in opposite directions and collide in the LSPCW. Since slow-light pulses in the LSPCW have quasilight velocities of $0.01c$–$0.1c$, a Doppler shift much larger than that obtained by acoustic waves is expected when the signal pulse is reflected by a mirror effectively formed by the control slow-light pulse.

In this study, we first explain the principle of mirror formation and the fundamental theory of the Doppler shift of light reflected in the photonic lattice. Next, we show the finite-difference time-domain (FDTD) simulation of spectral shifts that both agree and disagree with Doppler theory. We clarify the boundary condition between the agreement and disagreement by considering the adiabatic wavelength conversion [5–7,9–15] that occurs at the reflection, which comprehensively explains the behaviors of the spectral shifts.

II. THEORY

Figure 1 shows the schematic system considered herein. The LSPCW has a cutoff of the guided mode at the band edge. The signal pulse, set at frequency ω_{in} near the band edge, propagates from left to right. The intense control pulse at a telecom wavelength propagates in the Si LSPCW from right to left and produces TPA-induced carrier plasma. It reduces the refractive index of the LSPCW and shifts the photonic band gap (PBG) to the high-frequency side. In a simple consideration, this region would act as a mirror because the signal pulse is prohibited from propagating into this region and is reflected. (Later, we will discuss the fact that the reflection occurs only when the mirror satisfies a particular condition.) The carrier lifetime in the Si LSPCW has been measured to be 120 ps [5], which is much longer than durations of the signal and control pulses (we consider them to have a duration of several picoseconds). Therefore, the track of the control pulse turns into a uniform mirror whose front end moves with the control pulse. Consequently, the signal pulse is reflected, producing the Doppler shift.

Let us review the fundamental theory of the Doppler shift in the photonic lattice using the photonic band diagram of the guided mode (Fig. 2). Because of the periodicity of the photonic crystal, the band is symmetric at the wave number $k = \pm 0.5$ in the unit of $2\pi/a$, where a is the lattice constant. The signal pulse is initially propagating forward, and k is expressed as $k_{\mathrm{in}} + G$, where $0.5 \leqslant k_{\mathrm{in}} \leqslant 1.0$, and $G = \pm q$ (q is the integer number) is the reciprocal lattice vector, also with units of $2\pi/a$ [16]. In this range of k_{in}, the band slope is positive, indicating a positive group velocity. Figure 2 displays the operating points for $G = 0$ and $G = -1$. The frequency of the signal pulse, ω_{m}, which is observed by the mirror, suffers from the Doppler shift due to the moving mirror with velocity

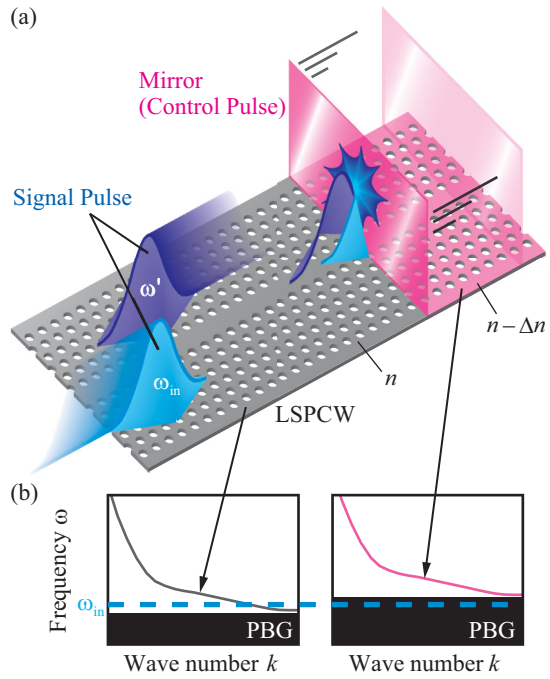

FIG. 1. Reflection and Doppler shift of a signal pulse at a moving mirror formed by the control pulse in LSPCW. (a) Schematic. (b) Photonic band of guided mode (solid line) and PBG (black region) before (left) and after (right) the mirror passes through.

$\upsilon_m(<0)$ and is given by

$$\omega_m = \omega_{in} - \upsilon_m(k_{in} + G). \tag{1}$$

The mirror is also considered as a moving light source that emits light at ω_m. The emitted light frequency ω' is then given by [17]

$$\omega' = \omega_m + \upsilon_m(k - G_s) \tag{2}$$

for another reciprocal lattice vector G_s. This corresponds to the final Doppler shift after the reflection. The wave number of the backward propagating wave after the reflection is in the range of $-1.0 \leqslant k \leqslant -0.5$. Defining $G_r = G + G_s$, Eqs. (1) and (2) give the following equation [4]:

$$\omega' = \omega_{in} + \upsilon_m(k - k_{in} - G_r). \tag{3}$$

This equation is expressed by the oblique lines with the slope of υ_m in Fig. 2. The intersections of the lines and bands with negative slopes (indicating a negative group velocity) correspond to the allowable operating points of the reflected signal pulse. We can expect multiple ω' for different G_r. Qualitatively, this phenomenon arises from the periodic behaviors of the reflection spectrum in the periodic structure [3].

III. CALCULATION

In the FDTD simulation, the LSPCW with the lattice shift in the third row from the line defect was modeled [5–7]. We assumed an effective slab index of $n = 2.963$ (modal equivalent index of a slab waveguide comprising a Si core with an index of 3.5 and a thickness of 260 nm and air cladding at $\lambda = 1550$ nm), an air hole index of 1.0, a lattice constant of $a = 440$ nm, a hole diameter of $2r/a = 0.59$, and a normalized lattice shift of $s/a = 0.3$. The signal pulse is excited for the transverse electric polarization at one end of the LSPCW. As for the mirror, we assumed a region wherein the index is simply reduced by Δn, and its front end is linearly sloped from 0% to 100% of Δn within a time of $\tau = 500$ fs. This mirror propagates with a velocity of υ_m from another end toward the signal pulse. To simplify the simulation, we neglected the cross-sectional distribution and propagation loss of this mirror.

Figure 3 shows the spectra of the reflected signal pulse for different values of Δn and υ_m. Since they were observed near the excitation point, spectral peaks from both the excitation (black dashed line) and the reflected pulse were observed. The spectra indicated by the black and gray arrows indicate that the blueshift increases with $|\upsilon_m|$. Focusing only on the black arrows, we notice that the magnitude of the blueshift depends not on $|\Delta n|$ but instead on $|\upsilon_m|$, which is the fundamental property of the Doppler shifts. When $|\upsilon_m|$ increases, the Doppler peaks decrease and soon disappear, particularly for small values of $|\Delta n|$, which will be discussed later. The spectral widths of the Doppler shifts increase compared to their initial values because the initial broadening in k_{in} reflects

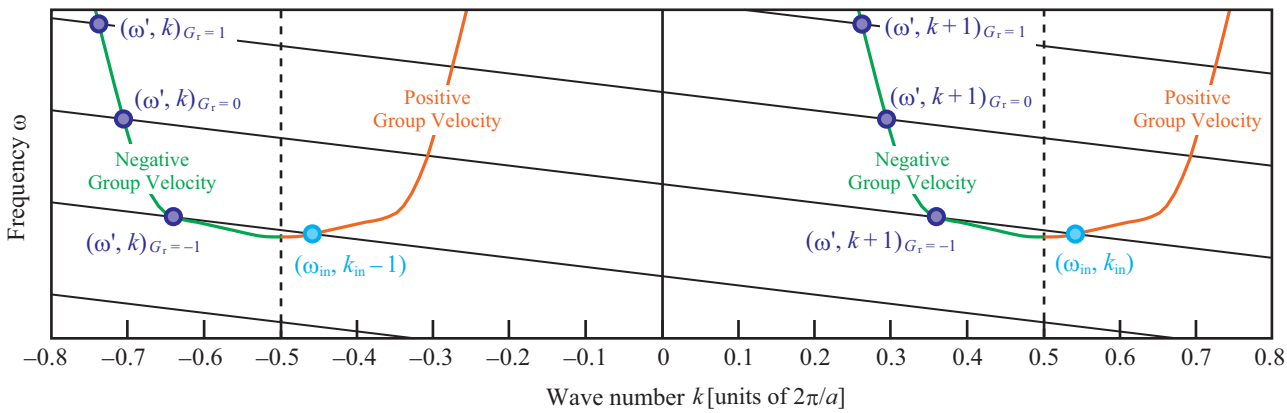

FIG. 2. Transition of the operating point of the signal pulse on photonic bands through the Doppler shift. Parallel oblique lines were obtained from Eq. (3).

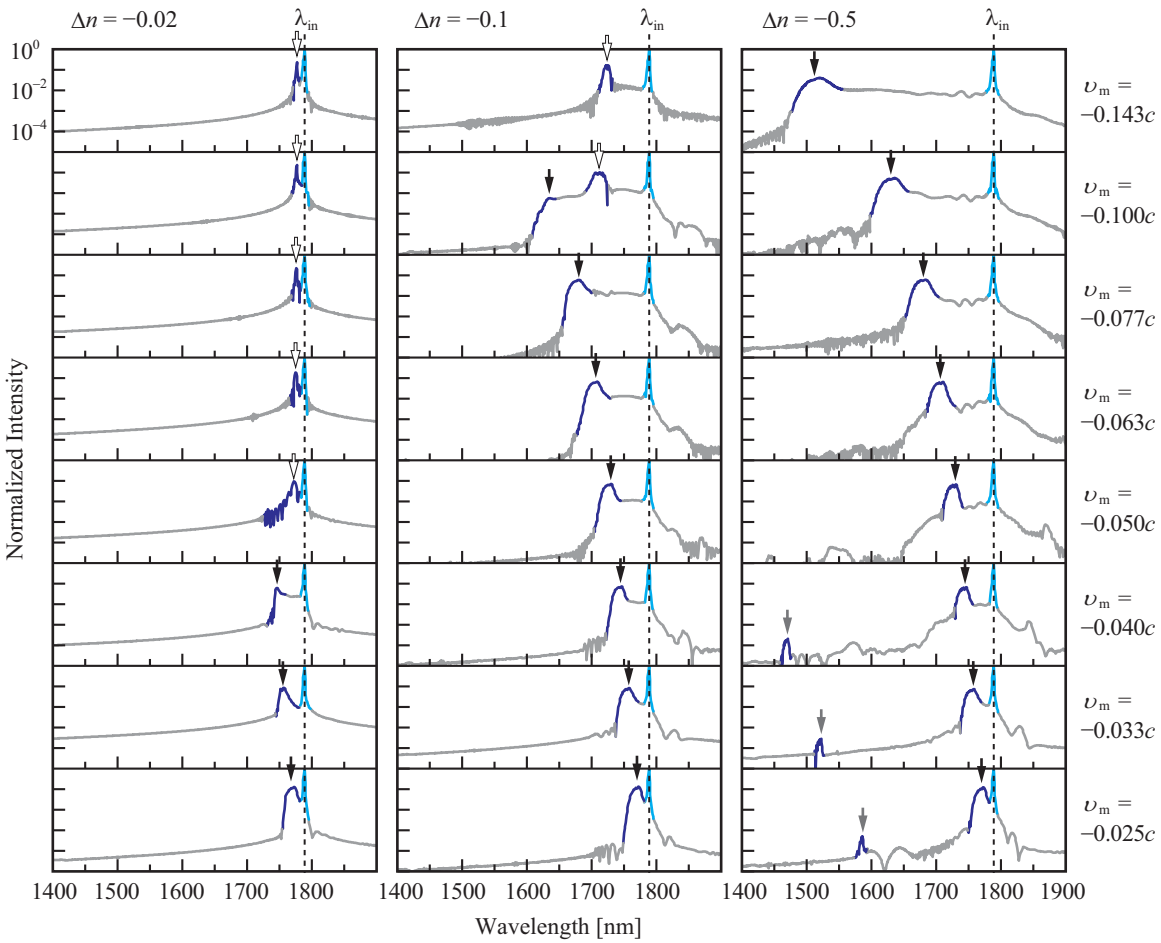

FIG. 3. Calculated signal spectra. Excitation is given around the wavelength centered at $\lambda = 1787$ nm, which corresponds to $k_{in} = 0.52$. c is the velocity of light in vacuum. The temporal full-width half-maximum of the initial pulse is 1.6 ps.

the broadening of the Doppler shift in accordance with Eq. (3). In calculating $\Delta\omega$ using Eq. (3), k_{in} was estimated from the field profile obtained in the FDTD simulation; in the LSPCW, a spatial beat with wave number Δk_{beat} appears in the pulse envelope due to the periodicity of the photonic band, and k_{in} is obtained from the relation $\Delta k_{beat} = 2k_{in} - 1$. The photonic band of the LSPCW needed to estimate k and ω' was independently calculated using the same parameters employed in the FDTD simulation. As shown in Fig. 4, the wavelength shifts $\Delta\lambda$ for $|\upsilon_m|$ obtained from the simulation and from Eq. (3) are in good agreement. The small difference might be caused by the errors in k_{in} and the band calculation. We are convinced that the main spectral peaks indicated by the black arrows and the subpeaks indicated by the gray arrows correspond to $G_r = -1$ and $G_r = 0$, respectively. The main peak has an intensity that is approximately 20 dB higher than that of the subpeak. This indicates that the Doppler shift for $G_r = -1$ is much more efficient than that for $G_r = 0$.

IV. DISCUSSION

As shown in Fig. 3, two Doppler peaks, for $G_r = 0$ and $G_r = -1$, appear when $|\Delta n|$ is large (e.g., $\Delta n = -0.5$). As shown by Fig. 2, the larger but less efficient shift for $G_r = 0$ is due to the discontinuous transition from the initial operating point to a point on the separate band. Thus, this shift is considered as a so-called nonadiabatic Doppler shift [3,4]. On the other hand, the smaller but more efficient shift for $G_r = -1$ occurs through the continuous intraband transition, suggesting some relevance with the adiabatic wavelength conversion process [4]. Figure 3 also shows that the intensity

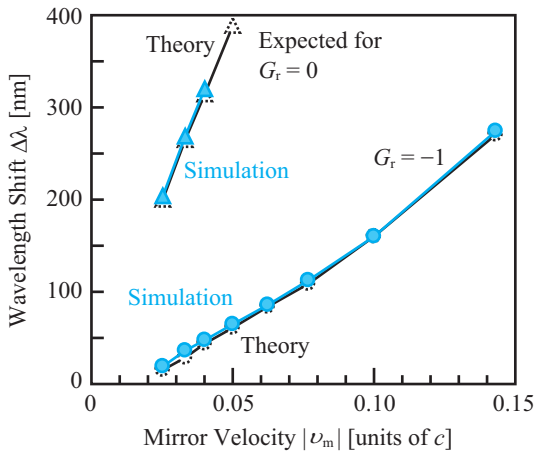

FIG. 4. Comparison of the wavelength shifts for υ_m obtained from FDTD simulation and Eq. (3) with $k_{in} = 0.52$.

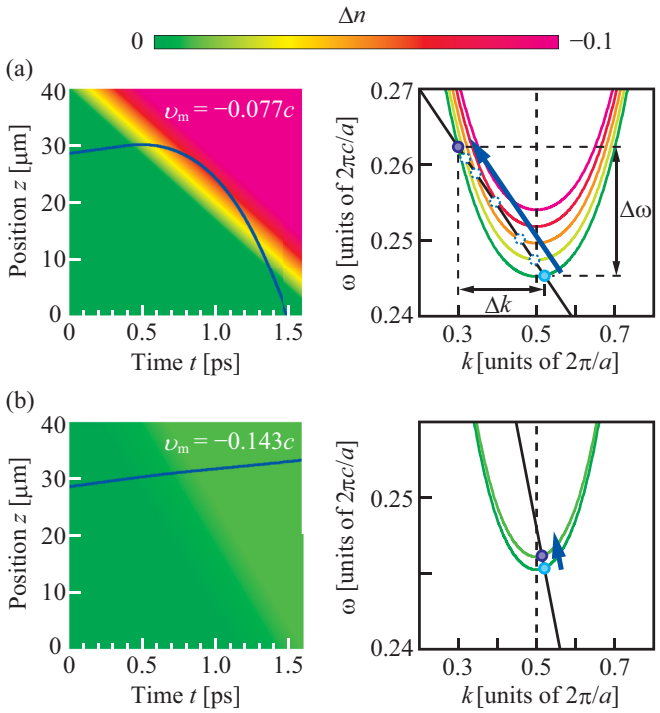

FIG. 5. Signal pulse trajectory (blue line) obtained using Eqs. (4) and (5) with spatiotemporal change in $|\Delta n|$ (color map of left panel) and transition of the operating point of the signal pulse in the photonic band, accounting for the corresponding frequency shift (right panel). (a) $\upsilon_m = -0.077c$ and maximum $|\Delta n|$ is 0.1. (b) $\upsilon_m = -0.143c$ and maximum $|\Delta n|$ is 0.01.

of the Doppler peak decreases when $|\Delta n|$ is small and $|\upsilon_m|$ is large, and other peaks that do not agree with the Doppler shift appear. They can also be explained by the adiabatic wavelength conversion.

The adiabatic frequency shift due to the index change $\Delta n(z,t)$ is given by [6]

$$\Delta\omega = \frac{\omega n_g \xi}{cn}\int_C \frac{\partial}{\partial t}\Delta n(z,t)dz = \frac{\omega\xi}{n}\int_C \frac{\partial}{\partial t}\Delta n(z,t)dt, \quad (4)$$

where z is position, t is time, n_g is the group index of the signal pulse, ξ is the dependence of the photonic-band frequency shift on the change in the index, and C is the trajectory of the signal pulse. Similarly, the wave number shift is given by

$$\Delta k = \frac{k_0 n_g \xi}{n}\int_C \frac{\partial}{\partial z}\Delta n(z,t)dz = \frac{k_0 c\xi}{n}\int_C \frac{\partial}{\partial z}\Delta n(z,t)dt. \quad (5)$$

The trajectory of the signal pulse can be obtained from these equations by setting the initial values of ω and k and assuming the index slope of the mirror to be $\Delta n(z,t) = \Delta n(-z/\upsilon_m - t)/\tau$. Figure 5 shows the resulting trajectory (left panel) and transition of the operating point in the photonic band (right panel). The color maps in the left panel depict the spatiotemporal movement of the mirror $|\Delta n|$ with υ_m.

First, we consider the situation that the signal pulse is completely reflected and the Doppler shift occurs. Fundamentally, the band shifts to the high-frequency side after passing through the front of the mirror and penetrating inside, and the operating point also shifts adiabatically with the band shift. Additionally, k shifts to the lower side, and the operating point thus moves along the black oblique line. When Δk is sufficiently large and the line crosses over the band edge ($k = 0.5$), the signal pulse begins to propagate in a backward direction, behaving as if it were reflected. Figure 5(a) shows the condition wherein the signal pulse begins to backpropagate in the index slope of the mirror and then returns to a position ahead of the mirror. Thus, the operating point moves to the high-frequency side of the initial band. From Eqs. (4) and (5), the following equation is obtained with the above Δn:

$$\frac{\Delta\omega}{\Delta k} = \int_C \frac{\partial}{\partial t}\Delta n(z,t)dt \Big/ \int_C \frac{\partial}{\partial z}\Delta n(z,t)dt = \upsilon_m. \quad (6)$$

Therefore, $\Delta\omega = \upsilon_m \Delta k$. This is in accordance with Eq. (3) because $\Delta k = k - k_{in} + 1$ in this consideration. This means that the black line depicting the adiabatic wavelength conversion in the right panel of Fig. 5(a) is the same as the

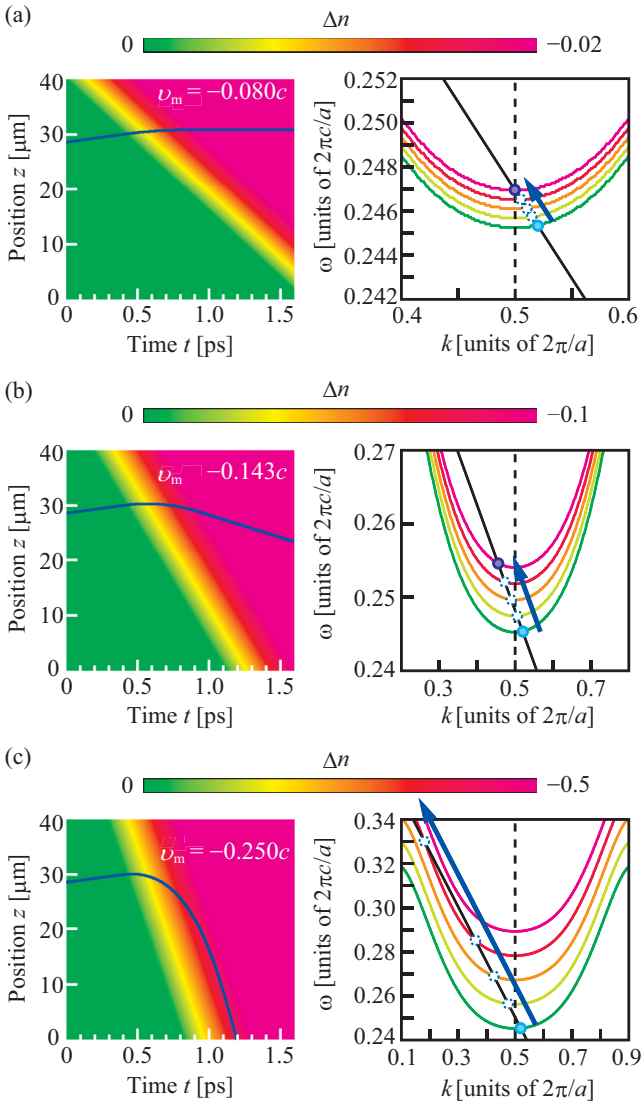

FIG. 6. Unique behaviors of a signal pulse under an incomplete-reflection condition, shown by the trajectory of signal pulse and transition of the operating point in the photonic band. (a) Stopping of the signal pulse. (b) A backpropagating signal pulse behind the mirror front. (c) Copropagation of a reflected signal pulse and mirror.

oblique line showing the Doppler shift in Fig. 2. Thus, the intraband Doppler shift is equivalent to the adiabatic wavelength conversion. However, such a Doppler shift occurs only when the signal pulse does not reach the end of the index slope and returns to a position ahead of the mirror. The band diagram in Fig. 5(a) indicates that the Doppler shift occurs more easily when the band shift is large ($|\Delta n|$ is large) and the oblique line is flatter (υ_m is low). This behavior suitably explains the ease of occurrence of the Doppler shifts indicated by the black arrows in Fig. 3.

Next, the situation where the signal pulse is not reflected is considered. When $|\Delta n|$ is small, the signal pulse reaches the end of the index slope, and when υ_m is high, the operating point does not cross over the $k = 0.5$ line. If these conditions are met simultaneously, the signal pulse will continue to propagate in the forward direction, as shown in Fig. 5(b). Considering some intermediate situations between Figs. 5(a) and 5(b), further unique behaviors of light propagation can be demonstrated. If $|\Delta n|$ is increased and/or υ_m is decreased slightly compared with those of Fig. 5(b), the operating point can terminate on the $k = 0.5$ line [Fig. 6(a)], where the signal pulse almost stops in the LSPCW. If $|\Delta n|$ and/or υ_m are changed further, the signal pulse backpropagates but cannot go ahead of the mirror without sufficient changes [Fig. 6(b)]. The spectral peaks indicated by the white arrows in Fig. 3 are produced in this way. If υ_m is carefully chosen such that the mirror and reflected signal pulse copropagate, the frequency shift becomes particularly large. This is because of the continuing interaction between the signal pulse and index change as long as the trajectory of the blueshifted signal pulse maintains the copropagating condition.

The frequency shifts for situations except for those shown in Fig. 5(a) are not considered for the reflection-type Doppler shift discussed so far. One may regard part of them as *extended* Doppler shifts induced by a moving dielectric boundary [18] because their ongoing shifts correspond to the straight line of the Doppler shift in the band diagram. However, the magnitude of the final shift also depends on the band shift determined by the index change $\Delta n(z,t)$, which is not the case for standard Doppler shifts. Therefore, they are better explained by the adiabatic wavelength conversion only or the extension of the cross-phase modulation discussed in Ref. [6].

V. CONCLUSION

We have discussed the reflection and Doppler shift in the signal slow-light pulse in a photonic-crystal waveguide, which is generated by the photonic band-gap shift induced by the nonlinearity of the control slow-light pulse. A wavelength shift of 10–150 nm is expected for the band-gap shift moving with a typical velocity of slow light ($0.01c$–$0.1c$ [19,20]). Engineering the group velocity is a particular capability of the photonic-crystal slow-light waveguide; thus, this approach has the potential to provide flexible wavelength conversion techniques. However, it requires a large index change of 0.01 to obtain an effective shift exceeding 30 nm, which is a challenge for experimental demonstrations. The index change based on the TPA-induced carriers in Si is limited by the TPA itself to the order of 0.001. The required index change is achievable using a semiconductor material such as InP, which exhibits more efficient carrier plasma dispersion [21]. Another candidate material is a chalcogenide glass, which produces an index change of $\sim$0.01 for a reasonable pulse peak power of less than 10 W through the huge optical Kerr effect [22].

We have also discussed the adiabatic wavelength conversion in detail and revealed that the efficient intraband Doppler shift is equivalent to the adiabatic wavelength conversion. We can also explain another shift by the adiabatic process, which does not reach the Doppler condition. We have clarified that the Doppler shift occurs more easily with a larger index change and a slower mirror.

ACKNOWLEDGMENTS

This work was partly supported by the New Energy and Industrial Technology Development Organization (NEDO), Japan.

[1] M. D. Thomson, S. M. Tzanova, and H. G. Roskos, Phys. Rev. B **87**, 085203 (2013).
[2] E. J. Reed, M. Soljacic, and J. D. Joannopoulos, Phys. Rev. Lett. **90**, 203904 (2003).
[3] E. J. Reed, M. Soljacic, and J. D. Joannopoulos, Phys. Rev. Lett. **91**, 133901 (2003).
[4] E. A. Ulchenko, D. Jalas, A. Y. Petrov, M. C. Muñoz, S. Lang, and M. Eich, Opt. Express **22**, 13280 (2014).
[5] K. Kondo, M. Shinkawa, Y. Hamachi, Y. Saito, Y. Arita, and T. Baba, Phys. Rev. Lett. **110**, 053902 (2013).
[6] K. Kondo and T. Baba, Phys. Rev. Lett. **112**, 223904 (2014).
[7] K. Kondo, N. Ishikura, T. Tamura, and T. Baba, Phys. Rev. A **91**, 023831 (2015).
[8] H. K. Tsang, C. S. Wong, and T. K. Liang, Appl. Phys. Lett. **80**, 416 (2002).
[9] M. F. Yanik and S. Fan, Phys. Rev. Lett. **92**, 083901 (2004).
[10] M. Notomi and S. Mitsugi, Phys. Rev. A **73**, 051803 (2006).
[11] S. F. Preble, Q. Xu, and M. Lipson, Nat. Photonics **1**, 293 (2007).
[12] Y. Tanaka, J. Upham, T. Nagashima, T. Sugiya, T. Asano, and S. Noda, Nat. Mater. **6**, 862 (2007).
[13] T. Kampfrath, D. M. Beggs, T. P. White, A. Melloni, T. F. Krauss, and L. Kuipers, Phys. Rev. A **81**, 043837 (2010).
[14] D. M. Beggs, T. F. Krauss, L. Kuipers, and T. Kampfrath, Phys. Rev. Lett. **108**, 033902 (2012).
[15] M. C. Muñoz, A. Y. Petrov, and M. Eich, Appl. Phys. Lett. **101**, 141119 (2012).
[16] D. Mori and T. Baba, Opt. Express **13**, 9398 (2005).
[17] C. Luo, M. Ibanescu, E. J. Reed, S. G. Johnson, and J. D. Joannopoulos, Phys. Rev. Lett. **96**, 043903 (2006).
[18] C. S. Tsai and B. A. Auld, J. Appl. Phys. **38**, 2106 (1967).
[19] S. A. Schulz, L. O'Faolain, D. M. Beggs, T. P. White, A. Melloni, and T. F. Krauss, J. Opt. **12**, 104004 (2010).
[20] T. Tamura, K. Kondo, Y. Terada, Y. Hinakura, N. Ishikura, and T. Baba, J. Lightwave Technol. **33**, 3034 (2015).
[21] B. R. Bennett, R. A. Soref, and J. A. D. Alamo, IEEE J. Quantum Electron. **26**, 113 (1990).
[22] K. Suzuki and T. Baba, Opt. Express **18**, 26675 (2010).